



## Research Article

# Adipose-derived stem cells inhibit dermal fibroblast growth and induce apoptosis in keloids through the arachidonic acid-derived cyclooxygenase-2/prostaglandin E2 cascade by paracrine

Jinxiu Yang<sup>1,2</sup>, Shiyi Li<sup>1,2</sup>, Leren He<sup>3,\*</sup> and Minliang Chen<sup>1,2,\*</sup>

<sup>1</sup>Department of Burn and Plastic Surgery, the Fourth Medical Centre, Chinese People's Liberation Army General Hospital, No. 51 Fucheng Road, Haidian District, Beijing, 100038, China, <sup>2</sup>Chinese People's Liberation Army General Hospital, No. 28 Fuxing Road, Haidian District, Beijing, 100853, China and <sup>3</sup>7th Department of Plastic Surgery, Plastic Surgery Hospital, Chinese Academy of Medical Sciences and Peking Union Medical College, No.33 Ba Dachu Road, Shi Jingshan District, Beijing, 100144, China

\*Correspondence. Minliang Chen, Email: chenml@sohu.com; Leren He, Email: heleren@sina.com

Received 19 August 2020; Revised 14 September 2020; Editorial decision 26 April 2021

## Abstract

**Background:** The clinical features of keloids consist of aberrant proliferation, secretion, differentiation and apoptosis of keloid dermis-derived fibroblasts (KFBs). Notably, the apoptosis rate of KFBs is lower than the proliferation rate. Though the anti-fibrotic effect of adipose-derived stem cells (ADSCs) on keloids has become a hot topic of research, the exact anti-fibrotic mechanism of the paracrine effect remains unclear. This study aimed to find out how the conditioned medium of ADSCs (ADSC-CM) exerts an anti-fibrotic effect in KFBs.

**Methods:** KFBs and ADSCs were extracted and cultured. Then, ADSC-CM was prepared. Whether ADSC-CM could inhibit KFB growth and induce apoptosis was verified by the use of a cell counting kit-8, an 5-Ethynyl-2-deoxyuridine (Edu) kit and flow cytometry. The expressions of cyclooxygenase-1 (COX-1), COX-2, caspase 3 and B-cell lymphoma-2 (Bcl-2) in ADSC-CM-cultured KFBs were tested by real-time PCR and western blotting. To clarify the role of COX-2 in ADSC-CM-induced KFB apoptosis, a specific COX-2 inhibitor, celecoxib, was applied to KFBs cultured in ADSC-CM. Moreover, we tested the production of arachidonic acid (AA) and prostaglandin E2 (PGE2) by ELISA. Then, we established a keloid transplantation model in a nude mouse to validate the therapeutic effect *in vivo*.

**Results:** The proliferation ability of KFBs cultured in ADSC-CM was found to be weakened and apoptosis was significantly increased. Caspase 3 expression was significantly upregulated and Bcl-2 was downregulated in ADSC-CM-cultured KFBs. Furthermore, ADSC-CM strikingly elevated COX-2 mRNA and protein expressions, but COX-1 expression was unaltered. COX-2 inhibitors reduced ADSC-CM-induced apoptosis. Additionally, COX-2 inhibition blocked the elevation of caspase 3 and reversed the decrease in Bcl-2 expression. ADSC-CM increased PGE2 levels by 1.5-fold and this effect was restrained by COX-2 inhibition. In the nude mouse model, expressions of AA, COX-2 and PGE2 were higher in the translated keloid tissues after ADSC-CM injection than in the controls.

**Conclusions:** We showed activation of the COX-2/PGE2 cascade in KFBs in response to ADSC-CM. By employing a specific COX-2 inhibitor, COX-2/PGE2 cascade activation played a crucial role in mediating the ADSC-CM-induced KFB apoptosis and anti-proliferation effects.

**Key words:** Keloids, Adipose-derived stem cells, Fibroblasts, Apoptosis, Anti-fibrosis, cyclooxygenase-2, Arachidonic acid

## Highlights

- The ADSC-CM activates the AA-COX-2/PGE2 cascade to inhibit growth of dermis-derived fibroblasts.
- ADSC-CM could strikingly elevate the expression of AA and then increase the expression of PGE2 in KFBs by selectively upregulating COX-2.
- ADSC-CM upregulated the expression of caspase 3 by KFBs, while Bcl-2 was downregulated.
- COX-2 inhibition could block the proliferation inhibition and induced apoptosis of KFBs cultured with ADSC-CM.

## Background

Keloids are benign dermal tumors with local infiltration characterized by abnormal proliferation of fibroblasts [1]. The entire process of keloid formation is associated not only with abnormal keloid dermis-derived fibroblast (KFB) proliferation but also with lower apoptosis rates. Apoptosis is thought to be vital in keloid formation [2].

Autologous fat transplantation is used to treat a variety of scars, including keloids. Previous studies have shown that autologous fat transplantation can improve the texture, softness and color of scars [3]. It has also been observed in histological studies that after the injection of adipose tissue around the scar tissue, the deposition of local fibrous tissue decreased and collagen fibers, which were previously disordered, became more similar to normal skin [4]. Researchers attribute this change to the anti-fibrotic effect of adipose-derived stem cells (ADSCs). Moreover, a growing number of scholars have confirmed that the paracrine signaling of ADSCs, i.e. the conditioned medium of ADSCs (ADSC-CM) [5–6], plays a decisive role in the anti-fibrotic effect. However, the specific anti-fibrotic mechanism of the ADSC paracrine pathway on the fibroblasts derived from scar dermis remains unclear.

Previous reports and our previous study, have shown that the content of fatty acids, especially arachidonic acid (AA) derived from polyunsaturated fatty acids, differs significantly between keloids and normal skin. The level of AA in keloids is significantly higher than in normal skin tissue [7]. Moreover, AA is closely related to inflammation occurrence. AA mediates the activation of the cyclooxygenase-2 (COX-2)/prostaglandin E2 (PGE2) inflammatory cascade and produces a variety of inflammation-related eicosanes, such as leukotrienes, prostanoids of prostaglandins (PGs), prostacyclins and thromboxanes [8]. Coincidentally, the occurrence of scarring is closely related to PGE2-related inflammation [9].

In this study, we found that ADSC-CM can affect KFBs through paracrine signaling by promoting their apoptosis and inhibiting their proliferation, thus exerting anti-fibrotic effects. First, ADSC-CM produces excessive AA by affecting the AA metabolic pathway of KFBs. Then, the AA-COX2/PGE2 inflammatory cascade increases the expression of pro-inflammatory factors in the metabolites, resulting in an increase in the apoptosis rate of KFBs and a decrease

in KFB proliferation. The possible mechanism of the anti-fibrotic effects of ADSC-CM through the AA-COX2/PGE2 pathway is detailed below.

## Methods

### Sample information

The investigative protocol was approved by the local ethics committee of the Fourth Medical Centre, Chinese People's Liberation Army General Hospital, and informed consent was obtained from each patient. Keloid samples and fat tissue were obtained from patients who underwent plastic surgery at the Plastic Surgery Hospital, Chinese Academy of Medical Sciences and Peking Union Medical College. Ultimately, a total of 15 keloid samples were collected.

### Fibroblast culture

Dermal tissues were washed 3 times with phosphate buffered saline (PBS) (Solarbio, China) and then minced into pieces (~1 mm). These pieces were explanted in Dulbecco's modified Eagle's medium (DMEM) (Gibco BRL, USA) containing 10% fetal bovine serum (FBS) (Gibco BRL, USA) and 1% penicillin/streptomycin (Bristol-Myers Squibb, USA) and incubated at 37°C in 5% carbon dioxide. The medium was changed every 3 days. After 7–10 days in the primary culture we confirmed that the cells had proliferated on the dish from the edge of the explanted tissue. Then, the cells were passaged 1–2 times per week.

### Human ADSC culture

The harvested fat tissue was digested in 0.1% collagenase type I on a shaker at 37°C for 45 minutes. Then, the stromal vascular fraction was filtered through a 70 µm porous filter (Millipore, USA) after centrifugation at 2000 rpm for 10 minutes. Next, the cell mass was resuspended in DMEM/F12 (Ham's F-12) medium containing 10% FBS and 1% penicillin/streptomycin and placed in a dish to be cultured at 37°C in an incubator with 5% carbon dioxide. The medium was changed every 3 days.

### Preparation of ADSC-CM

ADSCs in passage 3 to 8 that were 80–90% confluent were starved with a serum-free DMEM/F12 medium for 48 hours. Then, the ADSC supernatant was collected, centrifuged at

**Table 1.** Sequences for primers

Primer	Forward	Reverse
COX-1	TTTGGCATGAAACCCTACACCTC	TCCAACGCATCAATGTCTCCATA
COX-2	CTGGAACATGGAATTACCCAGTTTG	TGGAACATTTCCTACCACCAGCA
Bcl-2	TGGACAACCATGACCTTGGAC	GTGCTCAGCTTGGTATGCAGAA
Caspase 3	AAGGCAGAGCCATGGACCAC	CTGGCAGCATCATCCACACATAC
GAPDH	GCACCGTCAAGGCTGAGAAC	TGGTGAAGACGCCAGTGGGA

COX-1 cyclooxygenase-1, COX-2 cyclooxygenase-2, Bcl-2 B-cell lymphoma-2, GAPDH glyceraldehyde-3-phosphate dehydrogenase

3500 rpm for 10 minutes and filtered using a 0.22  $\mu$ m Millex-GP syringe filter (Millipore, USA) to ensure sterility. The product obtained was used as the ADSC-CM, which was stored at  $-80^{\circ}\text{C}$  until use. DMEM/F12 medium without FBS was used as the control medium. All the treatment groups were incubated for 48 hours.

#### Cell proliferation assay

Cell proliferation was determined by using the cell counting kit-8 (CCK-8) (Beyotime, China). Briefly, cells were seeded in 96-well plates at  $8 \times 10^3$  cells per well and incubated at  $37^{\circ}\text{C}$  for 24 hours. After synchronization with 100  $\mu$ L DMEM/F12 per well for 1, 2 and 3 days, 10  $\mu$ L of the CCK-8 solution was added to each well. The optical density was measured at 450 nm on a multiwell plate reader (Tecan, USA), and all samples were assayed in 6 replicates.

#### EdU cell proliferation

Cells were incubated for 48 hours with ADSC-CM or control medium. Using the BeyoClick™ EdU Cell Proliferation Kit with Alexa Fluor 488 (Beyotime, China) we identified the proliferating cells, which exhibited green fluorescence under a fluorescence microscope, and the nuclei were stained blue.

#### Annexin V Fluorescein isothiocyanate (FITC) and phycoerythrin double staining

Cells were incubated for 48 hours with ADSC-CM or control medium. Apoptotic cells were identified by the Annexin V FITC Apoptosis Detection Kit (BD Biosciences, USA) in accordance with the manufacturer's instructions. The flow cytometric analysis was performed immediately after supravital staining.

#### RT-PCR

A TRIzol reagent kit (Invitrogen, USA) was used for RNA extraction. The isolated RNA was reverse transcribed into complementary DNA using the Prime Script RT Reagent Kit (Takara, China). The primers (Takara, China) were synthesized for later use. Quantitative PCR was performed using the CFX96™ real-time system (Bio-Rad, USA) and SYBR Premix Ex Taq II (Takara, China) in 12  $\mu$ L PCR solution. The primer sequences are listed in Table 1. The results were normalized against the mean Cycle threshold (Ct) values of glyceraldehyde-3-phosphate dehydrogenase (GAPDH) using the  $\Delta\text{Ct}$  method, i.e.  $\Delta\text{Ct} = \text{Ct gene of interest} - \text{mean Ct}$

(GAPDH). The fold increase was calculated as  $2^{-\Delta\Delta\text{Ct}}$ . As a housekeeper gene, the expression of GAPDH in the same cell or tissue is generally constant, so it is used as an internal reference. Ct is the number of cycles that the fluorescence signal in each reaction tube goes through when it reaches the set threshold.

#### Western blot analysis

Radioimmunoprecipitation assay buffer (Beyotime, China) was used to lyse cells for 30 minutes on ice. The cells were then centrifuged at  $14,000 \times g$  at  $4^{\circ}\text{C}$  to remove the cell debris. Tissue samples were minced into pieces, ground under liquid nitrogen and centrifuged for 10 minutes at  $7500 \times g$  to obtain the supernatant. Samples containing 40 mg of protein were loaded onto a 5–10% polyacrylamide gel, separated by electrophoresis and transferred to a polyvinylidene difluoride membrane. The markers were tested by exposing the membranes to primary antibodies (Santa, USA). Horseradish peroxidase-conjugated goat anti-mouse/rabbit antibodies (Epizyme, China) were used as the secondary antibodies. The proteins were visualized with an enhanced chemiluminescence system using a Bio-Rad Gel Doc XR+ (Bio-Rad, USA). The blots were imaged using Image Lab™ software, version 5.1 (Bio-Rad, USA).

#### Enzyme immunoassay

The cell culture medium was centrifuged for 10 minutes at 3500 rpm. The concentrations of AA (Enzyme-linked Biotechnology, China) and PGE2 (Cayman Chemicals, USA) were determined by enzyme immunoassay according to the manufacturer's instructions.

#### Immunohistochemistry

Sections were rinsed with water and blocked with 10% normal goat Immunoglobulin G (IgG) for 20 minutes. Samples were incubated overnight at  $4^{\circ}\text{C}$  in primary mouse monoclonal anti-COX-2 antibodies (Santa Cruz Biotechnology, USA) diluted 1:200 in blocking solution. Slides were washed in PBS and subsequently incubated for 20 minutes in distilled  $\text{H}_2\text{O}$  with 3% hydrogen peroxide. Biotin-conjugated anti-mouse IgG (ZSGQ-BIO, China) was added for 20 minutes at room temperature. Diaminobenzidine (DAB) reagent (Beyotime Biotechnology, China) was applied for 2–3 minutes and hematoxylin (Beyotime Biotechnology, China) was applied for 2 minutes to re-stain the nuclei.

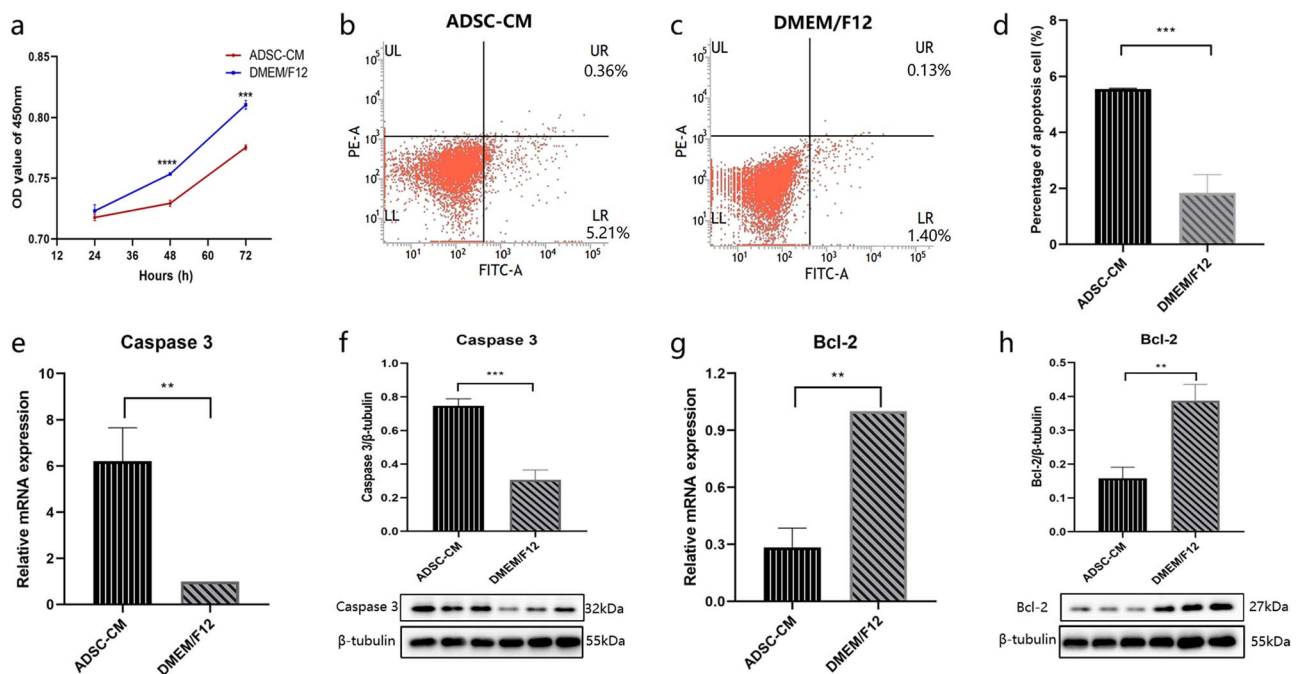


**Figure 1.** ADSC-CM inhibited KFB growth and induced KFB apoptosis. **(a)** Cell growth curve of KFBs in ADSC-CM and control groups (DMEM/F12),  $n = 6$ . **(b, c, d)** Apoptosis was assessed by Annexin V FITC and phycoerythrin staining in mesangial cells,  $n = 4$ . **(e, f)** The mRNA and protein levels of caspase 3 were assessed by RT-PCR and western blotting, respectively,  $n = 3$ . **(g, h)** The mRNA and protein levels of Bcl-2 were assessed by RT-PCR and western blotting, respectively,  $n = 3$ .  $**p < 0.01$ ,  $***p < 0.001$ ,  $****p < 0.0001$  (ADSC-CM vs DMEM/F12). ADSC-CM conditioned medium of adipose-derived stem cells, DMEM Dulbecco's modified Eagle's medium, KFBs keloid dermis-derived fibroblasts, OD optical density, F12 Ham's F-12, Bcl-2 B-cell lymphoma-2, LR viable apoptotic cells, UR non-viable apoptotic cells, UL debris and damaged cells, LL normal cells, FITC Fluorescein isothiocyanate

### A nude mouse model of *in vivo* transplantations of keloid

A model of keloid transplantation into nude mice (BALB/c-nu, 6–8 weeks) was established. Each nude mouse was transplanted 4 keloid tissues (1.0 cm × 0.6 cm). The keloid transplanted tissues were stable after 4 weeks. Next, we injected 0.1 mL of ADSC-CM into the keloid tissue once every 7 days for two weeks, while the control group was injected with an equal volume of DMEM/F12. Four weeks after the first treatment, we collected the translated keloid tissue after injection. The transplanted tissue collected was immediately stored in the  $-80^{\circ}\text{C}$  refrigerator for later use. We detected the expression of AA, COX-2 and PGE2 of the translated keloids to verify the *in vitro* change.

### Statistical analysis

The data were analysed using GraphPad Prism software 8.0 (GraphPad Software, Inc). Student's *t*-tests at a significance level of 5% were used to determine statistically significant differences between the 2 groups. One-way analysis of variance with *post hoc* test was used in more than 2 groups.

## Results

### ADSC-CM inhibited KFB growth and induced KFB apoptosis

The immunophenotype of ADSCs was examined by flow cytometry (Figure S1). Moreover, oil red O staining, alizarin

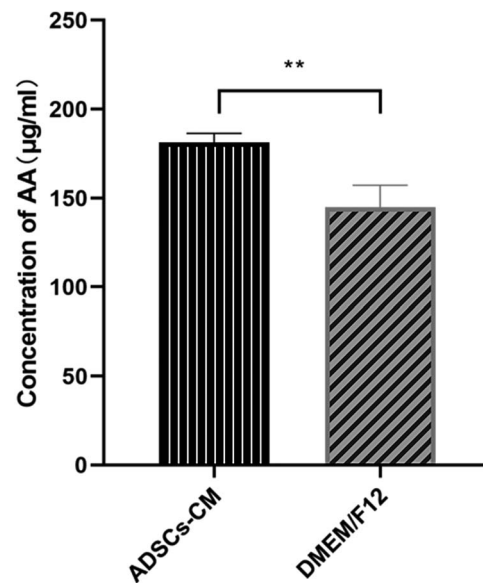


**Figure 2.** The expression of AA in keloid dermis-derived fibroblasts. The AA concentration in cell culture medium was determined by the ELISA kit.  $**p < 0.01$  vs control group (DMEM/F12 group),  $n = 6$ . AA arachidonic acid, ADSC-CM conditioned medium of adipose-derived stem cells, DMEM Dulbecco's modified Eagle's medium, ELISA enzyme-linked immunosorbent assay, F12 Ham's F-12

red S staining and alcian blue staining confirmed adipogenic differentiation (Figure S2), osteogenic differentiation (Figure S3) and chondrogenic differentiation (Figure S4) of

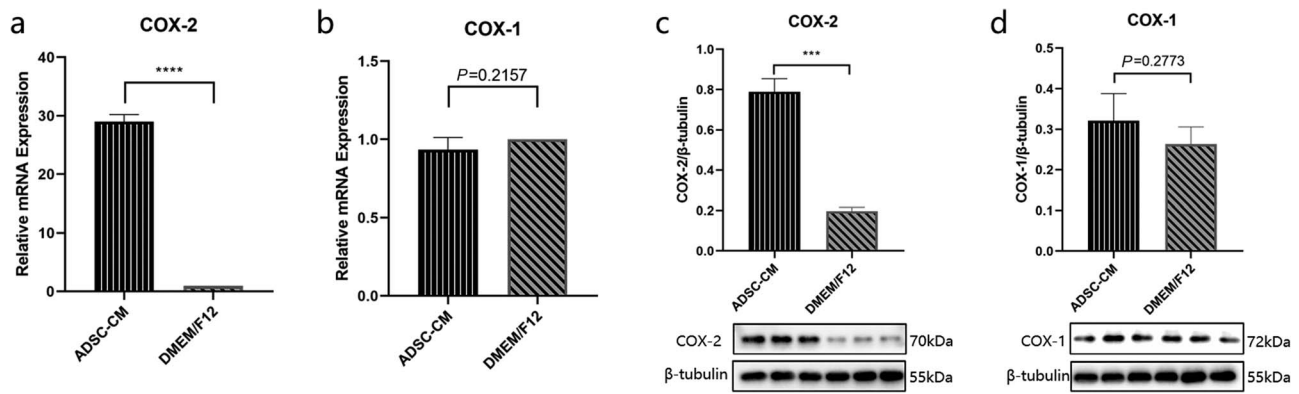


**Figure 3.** The expression of COX-2 and COX-1 in keloid dermis-derived fibroblasts cultured in ADSC-CM. **(a, b)** The mRNA expression of COX-2 and COX-1 determined by RT-PCR. **(c, d)** The protein expression of COX-2 and COX-1 were examined by western blotting. \*\*\* $p < 0.001$  vs control, \*\*\*\* $p < 0.0001$  vs control (DMEM/F12 group),  $n = 3$ . ADSC-CM conditioned medium of adipose-derived stem cells, COX-1 cyclooxygenase-1, COX-2 cyclooxygenase-2, DMEM Dulbecco's modified Eagle's medium, F12 Ham's F-12

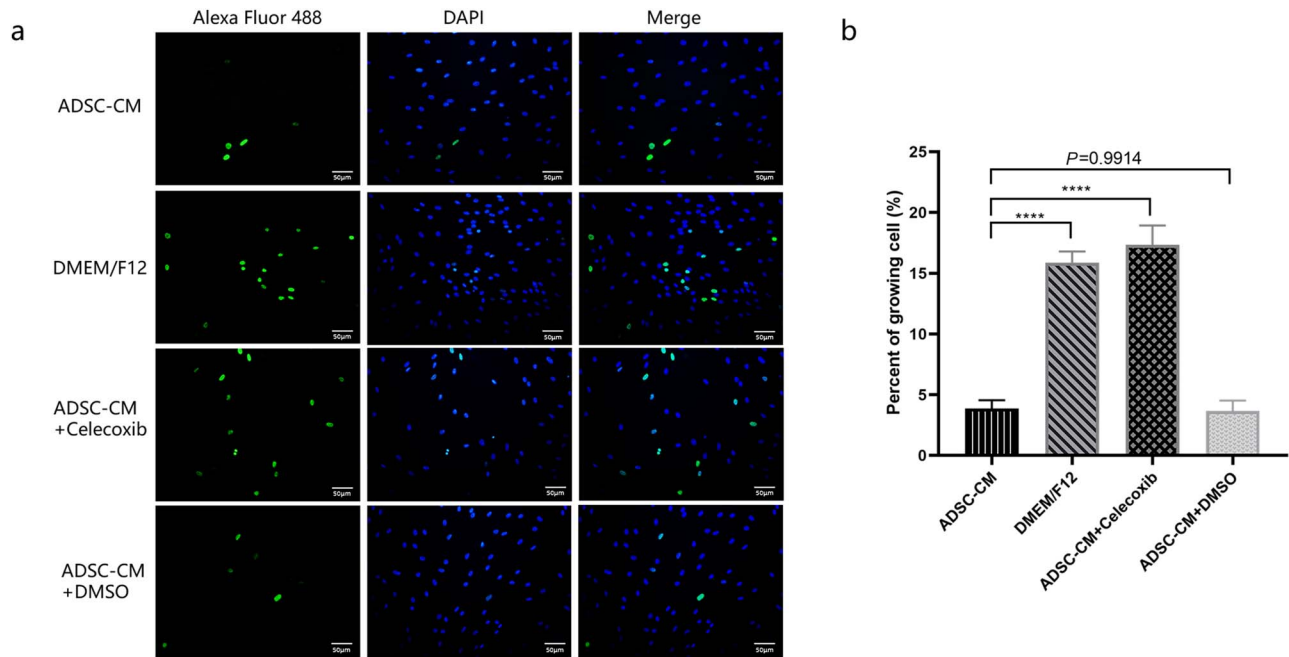


**Figure 4.** Inhibiting COX-2 promoted growth of ADSC-CM-induced KFBs. **(a)** Proliferating cells were identified by Alexa Fluor 488-stained. The proliferating cells exhibited green fluorescence under a fluorescence microscope and the nuclei were stained blue (Scale bar: 50  $\mu\text{m}$ ). **(b)** The percent of growing cells in each group, \*\*\*\* $p < 0.0001$  vs ADSC-CM group,  $n = 6$ . ADSC-CM conditioned medium of adipose-derived stem cells, DMEM Dulbecco's modified Eagle's medium, DMSO dimethyl sulfoxide, DAPI 4,6-diamino-2-phenyl indole, F12 Ham's F-12

ADSCs. To determine whether ADSC-CM could inhibit KFB growth, we cultured KFBs with ADSC-CM for 72 hours and tested their proliferation ability using the CCK-8 assay. As expected, ADSC-CM impaired the proliferative ability of KFBs compared to the control medium, with the strongest inhibitory effect at 48 hours (Figure 1a).

To investigate whether ADSC-CM could induce KFB apoptosis, we cultured KFBs with ADSC-CM and evaluated the apoptosis by analysing the proportion of apoptotic cells

(flow cytometry) and the mRNA and protein expressions of Bcl-2 and caspase 3. After 48 hours, cell apoptosis in the KFBs cultured with ADSC-CM was significantly increased (Figure 1b, c, d). Consistent with this result, the expression of caspase 3 in the KFBs cultured with ADSC-CM was significantly increased (Figure 1e, f) but Bcl-2 expression was decreased (Figure 1g, h). The above results indicate that ADSC-CM can trigger apoptosis and inhibit growth of KFBs.

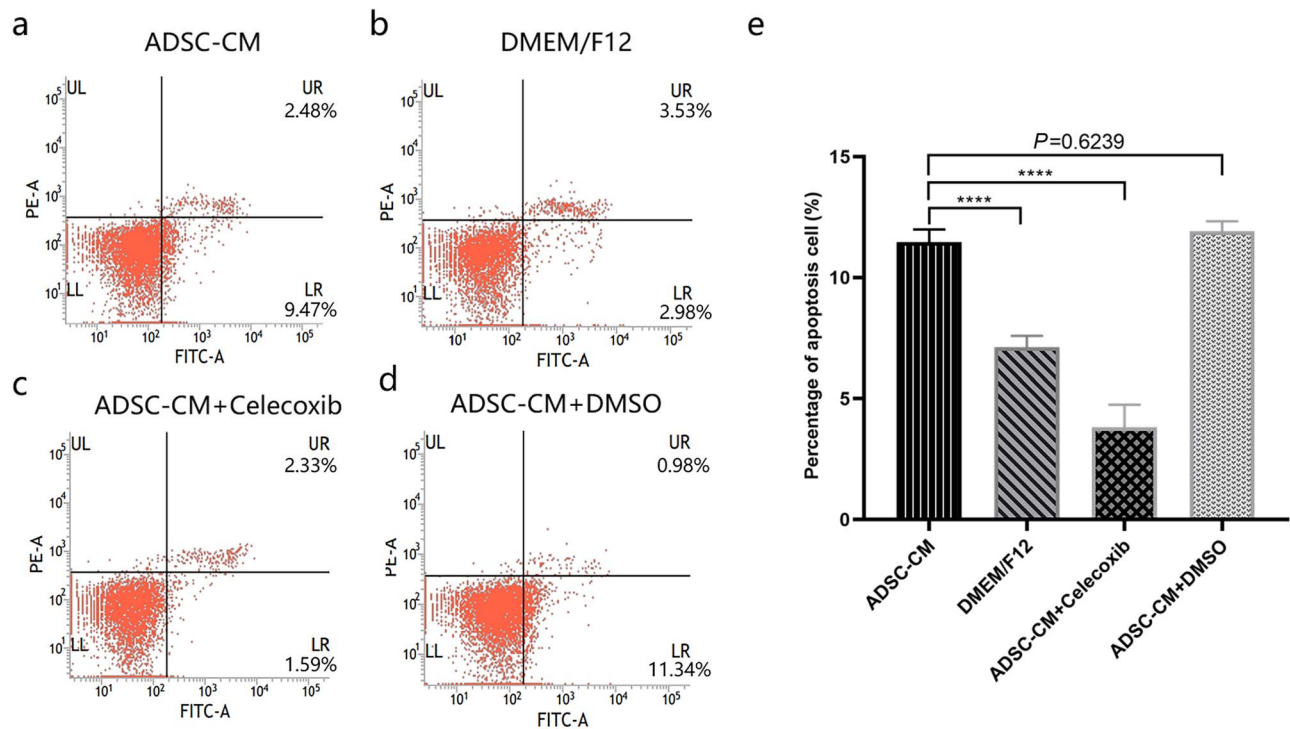


**Figure 5.** COX-2 inhibition ameliorated cell apoptosis induced by ADSC-CM. (a, b, c, d) The apoptosis was assessed by Annexin V FITC and phycoerythrin staining in mesangial cells by flow cytometric analysis. (e) The percentage of apoptotic cells in keloid dermis-derived fibroblasts cultured in ADSC-CM with or without COX-2 inhibition, \*\*\*\* $p < 0.0001$  vs ADSC-CM group,  $n = 4$ . ADSC-CM conditioned medium of adipose-derived stem cells, COX-2 cyclooxygenase-2, DMEM Dulbecco's modified Eagle's medium, DMSO dimethyl sulfoxide, F12 Ham's F-12, Bcl-2 B-cell lymphoma-2, LR viable apoptotic cells, UR non-viable apoptotic cells, UL debris and damaged cells; LL normal cells; FITC fluorescein isothiocyanate

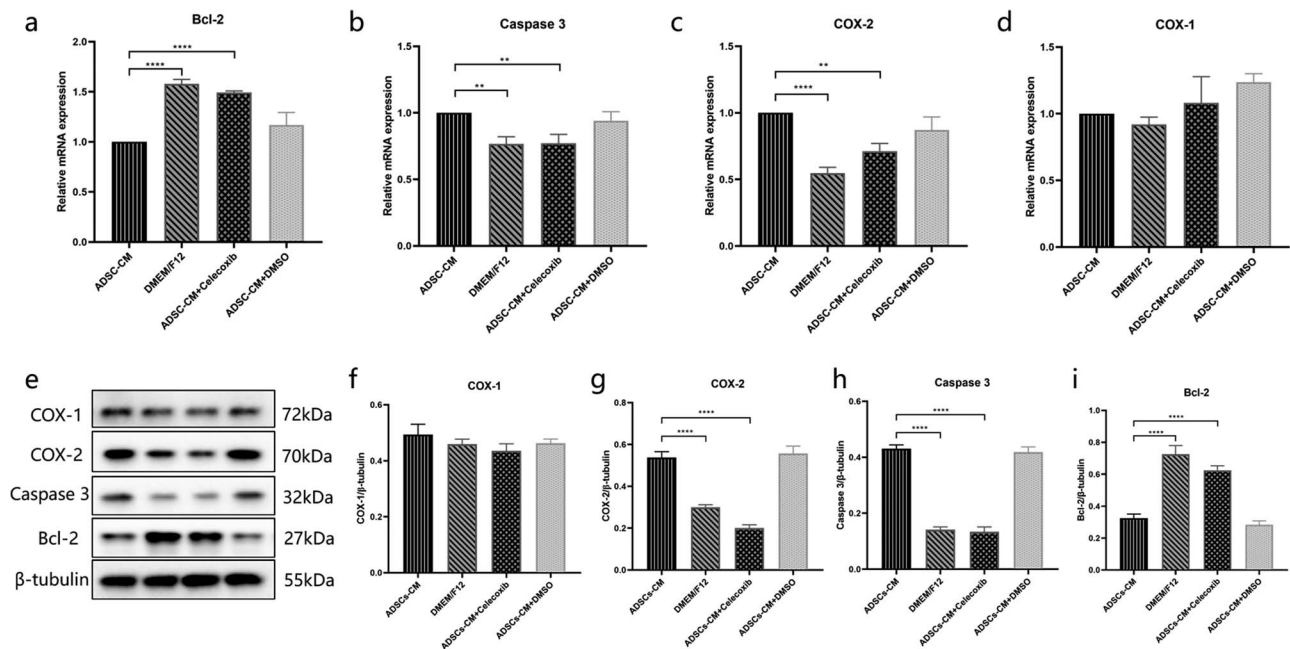


**Figure 6.** Inhibiting COX-2 blocked ADSC-CM-induced KFB apoptosis. (a, b, c, d) The mRNA expression of Bcl-2, Caspase 3, COX-2 and COX-1 were detected by RT-PCR in KFBs cultured in ADSC-CM with or without COX-2 inhibition. (e, f, g, h, i) The protein expression of Bcl-2, Caspase 3, COX-2 and COX-1 were examined by western blotting in KFBs cultured in ADSC-CM with or without COX-2 inhibition. \*\* $p < 0.01$ , \*\*\* $p < 0.001$ , \*\*\*\* $p < 0.0001$  vs ADSC-CM group,  $n = 3$ . ADSC-CM conditioned medium of adipose-derived stem cells, COX-1 cyclooxygenase-1, COX-2 cyclooxygenase-2, DMEM Dulbecco's modified Eagle's medium, DMSO dimethyl sulfoxide, KFBs keloid dermis-derived fibroblasts, F12 Ham's F-12; Bcl-2 B-cell lymphoma-2

### ADSC-CM enhanced the expression of AA in KFBs

The ELISA kit was used to measure the concentration of arachidonic acid, the initial substance of the AA-COX-2/PGE2 cascade. As shown in Figure 2, ADSC-CM increased the concentration of AA in KFBs by 1.25-fold. This indicates an induction of AA in response to the treatment of KFBs with ADSC-CM.

### ADSC-CM enhanced the expression of COX-2 in KFBs

We detected the expression of cyclooxygenase-1 (COX-1) and COX-2 in KFBs cultured in ADSC-CM. As shown in Figure 3a, ADSC-CM strikingly elevated COX-2 mRNA expression in the KFBs. However, the expression of COX-1 was unaltered (Figure 3b). We further examined the protein expressions of COX-1 and COX-2 by western blotting. Uniformly, COX-2 expression was significantly upregulated while COX-1 expression was unchanged (Figure 3c, d). These results suggest that COX-2 in KFBs was elevated by ADSC-CM.

### Inhibiting COX-2 promoted ADSC-CM-induced KFBs growth

To test the impact of COX-2 on ADSC-CM-inhibited KFB growth, a specific COX-2 inhibitor, celecoxib, was applied to KFBs cultured in ADSC-CM. In order to eliminate the effect of the celecoxib solvent, the group of ADSC-CM with dimethyl sulfoxide (the same concentration as celecoxib) was specially set up. In the results of fluorescent staining by Alexa Fluor 488t, the green fluorescence presented the proliferating cells, while the blue fluorescence was the cell nucleus by 4',6-diamidino-2-phenylindole staining (Figure 4). We found that the COX-2 inhibitor could relieve the inhibiting effect of proliferation on ADSC-CM-cultured KFBs.

### Inhibiting COX-2 blocked ADSC-CM-induced KFB apoptosis

To verify the impact of COX-2 on ADSC-CM-induced KFB apoptosis, celecoxib, one of the specific COX-2 inhibitors, was used to KFBs cultured in ADSC-CM. As shown in Figure 5, the COX-2 inhibitor moderated the cell apoptosis induced by ADSC-CM. Moreover, it restrained the upregulation of caspase 3 and reduction of Bcl-2 at the mRNA and protein levels in the KFBs cultured in ADSC-CM with celecoxib (Figure 6a, b, c, d, e). Notably, the upregulation of COX-2 induced by ADSC-CM was blocked by celecoxib, not only at the mRNA level but also at the protein levels (Figure 6a, f, g). These results showed that COX-2 might have a significant effect in mediating the KFB apoptosis induced by ADSC-CM.

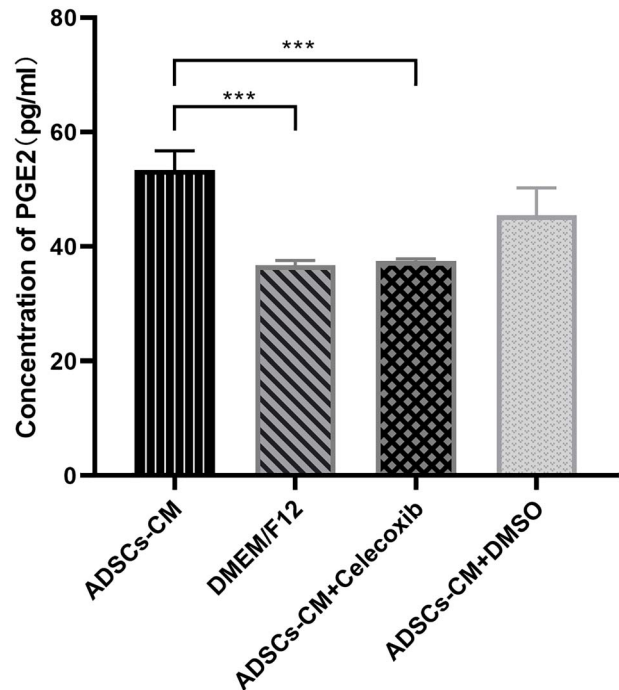


**Figure 7.** Inhibiting COX-2 blocked ADSC-CM-induced PGE2 production. The PGE2 concentration in cell culture medium was determined by the ELISA kit. \*\*\* $p < 0.001$  vs ADSC-CM group,  $n = 4$ . ADSC-CM conditioned medium of adipose-derived stem cells, COX-2 cyclooxygenase-2, DMEM Dulbecco's modified Eagle's medium, DMSO dimethyl sulfoxide, PGE2 prostaglandin E2, ELISA enzyme-linked immunosorbent assay, F12 Ham's F-12

### Inhibiting COX-2 blocked ADSC-CM-induced PGE2 production

To further test the effect of COX-2 inhibition in this experiment, we detected PGE2 production in the culture medium. We found that ADSC-CM could increase the PGE2 levels by 1.5-fold and that this effect was prevented by the COX-2 inhibitor (Figure 7). This demonstrated a COX-2-dependent induction of PGE2 in response to the treatment of KFBs with ADSC-CM.

### ADSC-CM exerted a therapeutic effect on transplanted keloid tissues

To further verify the therapeutic effect of ADSC-CM on keloids, we established a model of keloid transplantation into nude mice. We detected the expressions of AA, COX-2 and PGE2 involved in the transplanted keloid tissues after treatment to identify changes in the AA-derived COX-2/PGE2 cascade *in vitro*. As expected, the changes in these substances were consistent with those seen *in vitro*. As shown in Figures 8 and 9, the expressions of AA, COX-2 and PGE2 were higher in the tissues after ADSC-CM injection than in the control groups.

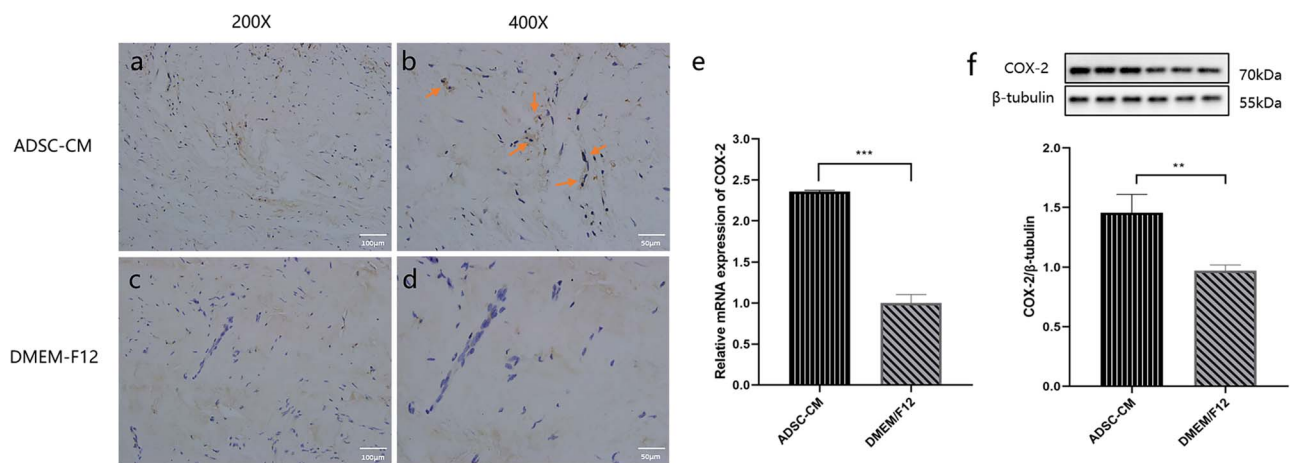


**Figure 8.** The expression of COX-2 involved in the transplanted keloid tissues after ADSC-CM treatment. (a, b, c, d) Digital photographs were taken for immunohistochemistry with COX-2 in the transplanted keloid tissues after being treated (magnification in a and c,  $\times 200$ ; in b and d,  $\times 400$ ). (e) The mRNA expression of COX-2 was detected by RT-PCR in transplanted keloid tissues after being treated. (f) The protein expression of COX-2 was examined by western blotting in transplanted keloid tissues after being treated.  $**p < 0.01$ ,  $***p < 0.001$  (ADSC-CM vs DMEM/F12),  $n = 6$ . ADSC-CM conditioned medium of adipose-derived stem cells, COX-2 cyclooxygenase-2, DMEM Dulbecco's modified Eagle's medium, F12 Ham's F-12

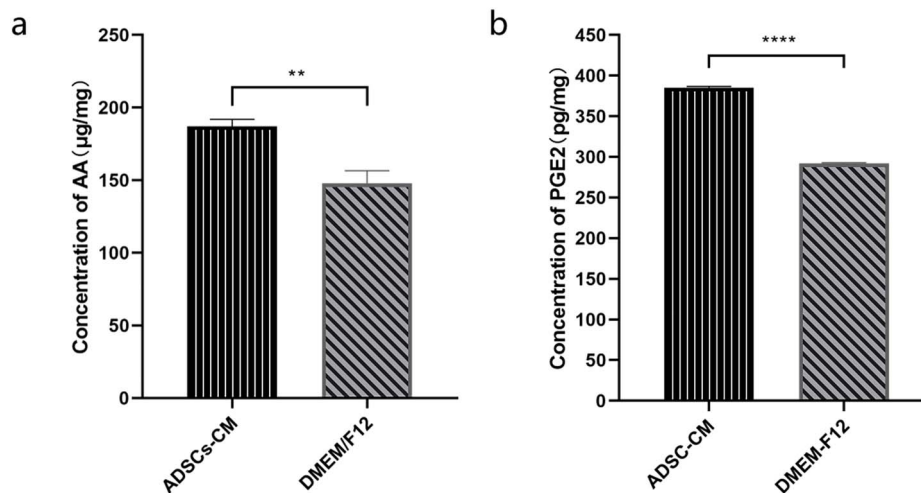


**Figure 9.** The expression of AA and PGE2 involved in the transplanted keloid tissues after ADSC-CM treatment. (a) The AA concentration in the transplanted keloid tissues after treatment was determined by the ELISA kit. (b) The PGE2 concentration in the transplanted keloid tissues after treatment.  $**p < 0.01$ ,  $****p < 0.0001$  (ADSC-CM vs DMEM/F12),  $n = 6$ . AA arachidonic acid, ADSC-CM conditioned medium of adipose-derived stem cells, DMEM Dulbecco's modified Eagle's medium, PGE2 prostaglandin E2, ELISA enzyme-linked immunosorbent assay, F12 Ham's F-12

## Discussion

Keloid, a kind of special scar, is formed through the abnormal and massive proliferation of fibroblasts from normal skin following trauma. Dermal-derived fibroblasts are the primary effector cells involved in keloid formation and are highly proliferative and resistant to apoptosis [10–11]. Moreover, fibroblasts are closely related to the development and clinical outcome of keloids [12–13]. Some have researchers inferred that, during keloid development, the anti-apoptotic capacity of KFBs could lead to the aberrant proliferation and extensive secretion of extracellular matrix [14].

Although the anti-fibrotic effects of ADSCs on keloids and KFBs have been recognized by most researchers, the signaling mechanisms responsible for these ADSC-induced anti-fibrotic

effects appear to be multifactorial, involving factors such as inflammation, immunology and oxidative stress [15]. The novel hypothesis proposed in this study is that ADSC-CM may be the key in the treatment of keloids with ADSCs. This is because it activates the AA-COX-2/PGE2 cascade to inhibit proliferation and initiate apoptosis of keloid-derived fibroblasts (Figure 10).

The apoptosis process, which may be activated by inflammatory factors and stress conditions, involves many signaling pathways and key factors [16]. Caspases are cysteine proteases that are activated by cleavage after aspartic acid residues [17]. Caspase 3 is one of the effector caspases and it ultimately leads to the destruction of cellular structure and DNA fragmentation [18]. Bcl-2 leads to the release of

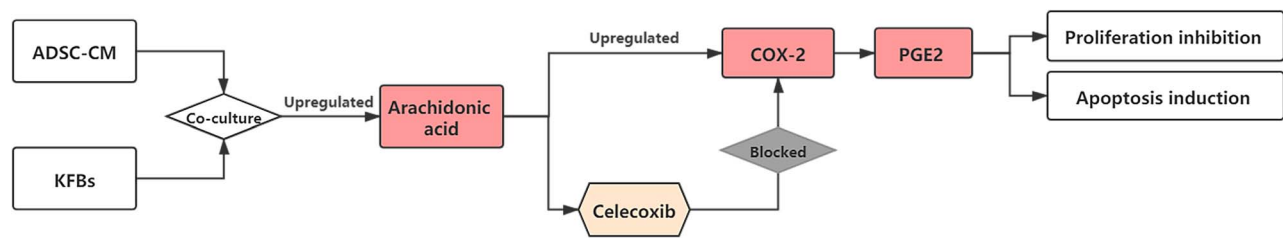


**Figure 10.** The response of KFBs to the ADSC-CM. ADSC-CM activates the AA-COX-2/PGE2 cascade to inhibit proliferation and initiate the apoptosis of keloid-derived fibroblasts, while the specific COX-2 inhibitors can block this process. AA arachidonic acid, ADSC-CM conditioned medium of adipose-derived stem cells, COX-2 cyclooxygenase-2, DMEM Dulbecco's modified Eagle's medium, KFBs keloid dermis-derived fibroblasts, PGE2 prostaglandin E2

Cytochrome C (cyt-c) from the mitochondria into the cytoplasm and it was the first anti-apoptotic gene to be identified [19]. In this study, we found that the expression of caspase 3 was higher in KFBs cultured with ADSC-CM for 48 hours, whereas that of Bcl-2 was lower. These data revealed that ADSC-CM can induce a high rate of apoptosis in KFBs.

Previous studies have shown that ADSCs induce apoptosis and inhibit proliferation in KFBs by paracrine effects [20], which is consistent with our findings. What is noteworthy in our study is that ADSC-CM induced only a 1-fold increase in apoptosis of KFBs compared to the effects of control media, whereas it reduced growing cells by 3-fold as assessed by Alexa Fluor 488. Thus, the effects of ADSC-CM on the inhibition of cell proliferation may be more prominent than on the induction of apoptosis. We assumed that ADSCs might induce KFB inhibition, in which the role of the AA-COX-2/PGE2 cascade is important.

Several studies have indicated that COX-2/PGE2 cascade activation is essential in the pathogenesis of many diseases. COX-2 and PGs, which are the results of COX-2 activity, mediate a variety of biological and pathological processes. Moreover, some researchers have suggested that the COX-2 pathway is involved in scar production in fetal skin and that targeting COX-2 may help limit scar formation in adult skin based on the scar-free healing that occurs in fetal skin during the first and second trimesters of development [21]. In keloid tissue, the abnormal expressions of COX-2 and PGE2 are potential risk factors for scar formation [22].

Cyclooxygenase has 2 isozymes. COX-2 is a key rate-limiting enzyme in PG synthesis and plays an important role in membrane phospholipid metabolism. In most normal tissues, COX-2 has a low baseline expression but can be induced to mediate inflammation and cell injury [23]; induction of COX-2 expression serves an important role in multiple pathophysiological processes. Metabolites and enzymes of the AA cascade, including the COX-2 enzyme and PGE2, are known to be critical mediators of the inflammatory response [21]. COX-2 has received much attention because of its involvement in diseases associated with inflammatory dysregulation [24]. Coincidentally, some significant inflammatory responses appear to be important for keloid formation.

COX-2 and PGE2 have various effects on cells depending on the type and origin of the cell. During the process of wound healing, the origin cell is the normal skin dermal-derived

fibroblast, while higher expression levels of COX-2 and PGE2 could stimulate the activation, migration and/or proliferation of these cells, augmenting scar tissue production [25]. Moreover, PGE2 is known to be able to reduce proliferation and collagen deposition by lung fibroblasts [26]. Cheng *et al.* reported that higher expression of COX-2 is accompanied by more hepatocyte apoptosis in nonalcoholic steatohepatitis [27]. In our study, we first examined the regulation of COX-2 in KFBs cultured in ADSC-CM. As expected, COX-2 and its product, PGE2, were remarkably elevated by ADSC-CM after 48 hours. To define the role of COX-2 in ADSC-CM-induced KFB apoptosis, a special COX-2 inhibitor, celecoxib, was applied to KFBs cultured in ADSC-CM. Notably, the COX-2 inhibitor strikingly blocked ADSC-CM-induced KFB apoptosis by blocking PGE2 production. When KFBs were cultured in ADSC-CM with COX-2 inhibitor, the KFB apoptosis was decreased and the proliferation was increased. Thus, we suggest that ADSCs might promote keloid dermal-derived fibroblast apoptosis via the AA-COX-2/PGE2 cascade.

The COX-2 inhibitors, as well as the celecoxib in our study, are known as nonsteroidal anti-inflammatory drugs and are reported to be used in wound healing. However, their impact on wound healing is highly controversial [28]. As shown in our study, the COX-2 inhibitors may have a negative effect on keloid treatment. The COX-2 inhibitor would block ADSC-CM-induced KFB apoptosis and promote KFB growth. Previous research has shown that, compared with normal fibroblasts, KFBs produce less PGE2 [29]. A consensus has been reached that the best method of prevention of burn scars is to apply compression. Coincidentally, this process induced an increase of PGE2 releasing, indicating the effect of PGE2-induced scar remission by pressure therapy [30]. Our study may verify this point by suggesting that ADSC-CM could inhibit KFBs by releasing a large amount of PGE2.

Moreover, in the study of wound healing, the target cells are fibroblasts derived from the dermis of normal skin (NFBS). Interestingly, with regard to proliferation, migration and apoptosis, there are different responses to the ADSC-CM of the KFBs and NFBS. In the *in vivo* animal study, ADSCs significantly reduced the wound size and accelerated re-epithelialization from the edge. In terms of apoptosis, a study by Wang [31] tried to determine the impact of ADSC-CM on damaged NFBS. The results showed that ADSC-CM

treatment could obviously decrease the apoptotic ratio in irradiated NFBs ( $p < 0.01$ ). These different effects of ADSC-CM on 2 kinds of fibroblasts are worthy of pondering.

Our study proved for the first time, through *in vitro* and *in vivo* studies, that ADSC-CM can induce KFB apoptosis by regulating the COX-2/PGE2 pathway, thereby exerting an anti-fibrotic effect on KFBs. Notably, our study focused on the inhibitory mechanism of ADSC-CM on fibroblasts. Given that a variety of bioactive substances can be secreted into ADSC-CM, the specific key factors in this study were not identified. Therefore, further research is needed to determine which components and factors in ADSC-CM, such as exosomes from ADSCs, may play a specific role in the anti-fibrotic effect and inhibition induction.

## Conclusions

In summary, in human keloid dermal-derived fibroblasts, we identified activation of the COX-2/PGE2 cascade in response to ADSCs. Furthermore, by employing a specific COX-2 inhibitor, celecoxib, we suspected that AA-induced COX-2/PGE2 cascade activation played a detrimental role in mediating ADSC-CM-induced KFB apoptosis and anti-proliferation effects. This pathway may act as a key contributor to the mechanism of the anti-fibrotic effect of ADSCs.

## Supplementary data

Supplementary data is available at *Burns & Trauma Journal* online.

## Acknowledgments

The authors would like to thank Mr. Kui Ma and Mrs. Ning Dong for their technical assistance.

## Funding

The current study was supported by grant from the National Natural Science Foundation of China (No. 81772085).

## Conflicts of interest

None declared.

## Abbreviations

AA: arachidonic acid; ADSC-CM: conditioned medium of adipose-derived stem cells; ADSCs: adipose-derived stem cells; COX-1: cyclooxygenase-1; COX-2: cyclooxygenase-2; DMEM: Dulbecco's modified Eagle's medium; FBS: fetal bovine serum; KFBs: keloid dermis-derived fibroblasts; NFBs: fibroblasts derived from the dermis of normal skin; PBS: phosphate buffered saline; PGE2: prostaglandin E2; PGs: prostaglandins.

## Ethics approval and consent to participate

The investigative protocol was approved by the local ethics committee of the Fourth Medical Centre, Chinese People's Liberation Army General Hospital.

## References

1. Jumper N, Paus R, Bayat A. Functional histopathology of keloid disease. *Histol Histopathol.* 2015;30:1033–57.
2. Tan S, Khumalo N, Bayat A. Understanding keloid pathobiology from a quasi-neoplastic perspective: less of a scar and more of a chronic inflammatory disease with cancer-like tendencies. *Front Immunol.* 2019;10:1810:1–15.
3. Xu X, Lai L, Zhang X, Chen J, Chen J, Wang F, *et al.* Autologous chyle fat grafting for the treatment of hypertrophic scars and scar-related conditions. *Stem Cell Res Ther.* 2018;9(1):64:1–8.
4. Chen J, Lai L, Ma K, Xu X, Huang Z, Zhou G, *et al.* The effect of chyle fat injection on human hypertrophic scars in an animal model: a new strategy for the treatment of hypertrophic scars. *Ann Plast Surg.* 2019;82:622–7.
5. Zhang W, Bai X, Zhao B, Li Y, Zhang Y, Li Z, *et al.* Cell-free therapy based on adipose tissue stem cell-derived exosomes promotes wound healing via the PI3K/Akt signaling pathway. *Exp Cell Res.* 2018;370:333–42.
6. Bajek A, Gurtowska N, Olkowska J, Kazmierski L, Maj M, Drewa T. Adipose-derived stem cells as a tool in cell-based therapies. *Arch Immunol Ther Exp (Warsz).* 2016;64:443–54.
7. Louw L. Keloids in rural black South Africans. Part 3: a lipid model for the prevention and treatment of keloid formations. *Prostaglandins Leukot Essent Fatty Acids.* 2000;63:255–62.
8. Calder PC. Omega-3 fatty acids and inflammatory processes: from molecules to man. *Biochem Soc Trans.* 2017;45:1105–15.
9. Hayashi T, Nishihira J, Koyama Y, Sasaki S, Yamamoto Y. Decreased prostaglandin E2 production by inflammatory cytokine and lower expression of EP2 receptor result in increased collagen synthesis in keloid fibroblasts. *J Invest Dermatol.* 2006;126:990–7.
10. Carantino I, Florescu IP, Carantino A. Overview about the keloid scars and the elaboration of a non-invasive, unconventional treatment. *J Med Life.* 2010;3:122–7.
11. Duan C, Chen K, Yang G, Li T, Liu L. HIF-1 $\alpha$  regulates Cx40-dependent vasodilatation following hemorrhagic shock in rats. *Am J Transl Res* 2017;9:1277–86.
12. Doong H, Dissanayake S, Gowrishankar TR, LaBarbera MC, Lee RC. The 1996 Lindberg award. Calcium antagonists alter cell shape and induce procollagenase synthesis in keloid and normal human dermal fibroblasts. *J Burn Care Rehabil.* 1996;17:497–514.
13. Philandrianos C, Kerfant N, Jaloux C, Jr, Martinet L, Bertrand B, Casanova D. Keloid scars (part I): clinical presentation, epidemiology, histology and pathogenesis. *Ann Chir Plast Esthet.* 2016;61:128–35.
14. Chen ZY, Yu XF, Huang JQ, Li DL. The mechanisms of  $\beta$ -catenin on keloid fibroblast cells proliferation and apoptosis. *Eur Rev Med Pharmacol. Sci* 2018;22:888–95.
15. Wang X, Ma Y, Gao Z, Yang J. Human adipose-derived stem cells inhibit bioactivity of keloid fibroblasts. *Stem Cell Res Ther.* 2018;9:40:1–8.

16. Zhang MZ, Liu YF, Ding N, Zhao PX, Zhang X, Liu MY, *et al.* 2-Methoxyestradiol improves the apoptosis level in keloid fibroblasts through caspase-dependent mechanisms in vitro. *Am J Transl Res.* 2018;10:4017–29.
17. Zhu S, Pabla N, Tang C, He L, Dong Z. DNA damage response in cisplatin-induced nephrotoxicity. *Arch Toxicol.* 2015;89:2197–205.
18. Mukherjee A, Williams DW. More alive than dead: non-apoptotic roles for caspases in neuronal development, plasticity and disease. *Cell Death Differ.* 2017;24:1411–21.
19. Roset R, Ortet L, Gil-Gomez G. Role of Bcl-2 family members on apoptosis: what we have learned from knock-out mice. *Front Biosci.* 2007;12:4722–30.
20. Liu J, Ren J, Su L, Cheng S, Zhou J, Ye X, *et al.* Human adipose tissue-derived stem cells inhibit the activity of keloid fibroblasts and fibrosis in a keloid model by paracrine signaling. *Burns.* 2018;44:370–85.
21. Wilgus TA, Bergdall VK, Tober KL, Hill KJ, Mitra S, Flavanhan NA, *et al.* The impact of cyclooxygenase-2 mediated inflammation on scarless fetal wound healing. *Am J Pathol.* 2004;165:753–61.
22. Abd El-Aleem SA, Abdelwahab S, Am-Sherief H, Sayed A. Cellular and physiological upregulation of inducible nitric oxide synthase, arginase, and inducible cyclooxygenase in wound healing. *J Cell Physiol.* 2019;234:23618–32.
23. Greenhough A, Smartt HJ, Moore AE, Roberts HR, Williams AC, Paraskeva C, *et al.* The COX-2/PGE2 pathway: key roles in the hallmarks of cancer and adaptation to the tumour microenvironment. *Carcinogenesis.* 2009;30:377–86.
24. Kim KN, Ko YJ, Yang HM, Ham YM, Roh SW, Jeon YJ, *et al.* Anti-inflammatory effect of essential oil and its constituents from fingered citron (*Citrus medica* L. var. *sarcodactylis*) through blocking JNK, ERK and NF- $\kappa$ B signaling pathways in LPS-activated RAW 264.7 cells. *Food Chem Toxicol.* 2013;57:126–31.
25. Wilgus TA, Vodovotz Y, Vittadini E, Clubbs EA, Oberyszyn TM. Reduction of scar formation in full-thickness wounds with topical celecoxib treatment. *Wound Repair Regen.* 2003; 11:25–34.
26. McAnulty RJ, Hernández-Rodríguez NA, Mutsaers SE, Coker RK, Laurent GJ. Indomethacin suppresses the anti-proliferative effects of transforming growth factor-beta isoforms on fibroblast cell cultures. *Biochem J.* 1997;321:639–43.
27. Cheng Q, Li N, Chen M, Zheng J, Qian Z, Wang X, *et al.* Cyclooxygenase-2 promotes hepatocellular apoptosis by interacting with TNF- $\alpha$  and IL-6 in the pathogenesis of nonalcoholic steatohepatitis in rats. *Dig Dis Sci.* 2013;58: 2895–902.
28. Su WH, Cheng MH, Lee WL, Tsou TH, Chang WH, Chen CS, *et al.* Nonsteroidal anti-inflammatory drugs for wounds: pain relief or excessive scar formation? *Mediators Inflamm.* 2010;2010:413238:1–8.
29. Yeh FL, Shen HD, Lin MW, Chang CY, Tai HY, Huang MH. Keloid-derived fibroblasts have a diminished capacity to produce prostaglandin E2. *Burns.* 2006;32:299–304.
30. Renò F, Grazianetti P, Cannas M. Effects of mechanical compression on hypertrophic scars: prostaglandin E2 release. *Burns.* 2001;27:215–8.
31. Wang T, Guo S, Liu X, Xv N, Zhang S. Protective effects of adipose-derived stem cells secretome on human dermal fibroblasts from ageing damages. *Int J Clin Exp Pathol.* 2015;8:15739–48.